Micromachined silicon plates for sensing molecular interactions

Edwin T. Carlen,[a] Marc S. Weinberg, Christopher E. Dubé,
Angela M. Zapata, and Jeffrey T. Borenstein
The Charles Stark Draper Laboratory, 555 Technology Square, Cambridge, Massachusetts 02139

(Received 30 June 2006; accepted 14 September 2006; published online 26 October 2006)

A micromachined surface stress sensor based on a thin suspended crystalline silicon circular plate measures differential surface stress changes associated with vapor phase chemisorption of an alkanethiol self-assembled monolayer. The isolated face of the suspended silicon plate serves as the sensing surface treated with a receptor layer sensitive to a target molecule, in this case Au(111). Chemisorption of an alkanethiol on the gold coated silicon surfaces results in plate bending. Plate displacements, measured with a phase scanning interferometer, indicate a differential surface stress change $\Delta\sigma_s=-0.72\pm0.02$ N m^{-1} for 1-dodecanethiol. © *2006 American Institute of Physics*. [DOI: 10.1063/1.2364878]

The measurement of surface stress has been pursued for many years and is a critical factor for understanding a wide variety of surface-related phenomena, for example, surface reconstruction, shape transitions in nanoscale particles, surface alloying, surface diffusion, epitaxial growth, and self-assembled domain patterns.[1,2] Macroscale structures have been used to measure crystal response,[3] vertical deflections of *AT*-cut quartz plates,[4] and to characterize thin-film properties of sputter deposited thin films.[5] More recently, microfabricated silicon and silicon nitride cantilever beams have been used to measure the change in differential surface stress induced by adsorption of biological materials on functionalized beam surfaces[6–8] and alkanethiols on Au(111) coated beams.[9–12] Surface stress sensing of conformational changes of biomolecules selectively bound to a receptor layer may provide a viable alternative to resonant based techniques, such as quartz crystal microbalances and resonant cantilever beams,[13–15] for label-free biosensing. The surface stress sensing mechanism is fundamentally different than resonant mass sensing, where the latter detect a change in resonant frequency due to adsorption on the resonator. The detection resolution of the resonant mass sensors is typically reduced in a liquid medium due to the reduction of the resonator quality factor caused by increased viscous damping by the liquid. Techniques have been developed to ameliorate this problem,[16,17] however, with increased complexity to the sensor. Surface stress sensors detect low frequency deflection changes of mechanical structures due to differential surface stress changes of a sensing surface. Therefore, the resolution of the surface stress sensors is minimally affected by viscous damping. Many questions still remain regarding the repeatability of surface stress sensing for different ligand-ligate systems and solution environments.

A mathematical description of surface stress has been previously defined as $\sigma_{s_{ij}}=\delta_{ij}\gamma+\partial\gamma/\partial\varepsilon_{ij}$,[18,19] where σ_s (N m^{-1}) is the surface stress, γ (J m^{-2}) is the surface free energy, and ε the strain. Tensor quantities can be represented as scalar quantities for surfaces with threefold, or larger, lattice symmetry [Au(111) has a threefold lattice symmetry]. In thin samples, surface stress can produce measurable elastic bending, such as the bending of the gold coated silicon plates due to the adsorption of an alkanethiol, presented in this letter.

From elasticity theory, the following assumptions are used in deriving small plate deflections due to a uniform axial surface stress: (a) the plate material is homogeneous with uniform thickness t, (b) $t<d/10$, where d is the plate diameter, (c) the maximum deflection $w_m<t/2$,[20,21] and (d) large deflection shearing forces Q_r and body forces not considered. Figures 1(a) and 1(b) show dimensions, forces, and moments. Assuming uniform axial stress on the plate surface $\sigma_s^+\neq\sigma_s^-$, a differential surface stress $\sigma_s=\sigma_s^+\delta(z-t/2)-\sigma_s^-\delta(z+t/2)$,[22] where δ is the Dirac-delta function, has the effect of generating a stress couple of radial flexure bending moment M, shown in Fig. 1(c). This is equivalent to applying a force F at the plate neutral surface n thus generating M at the clamped boundary such that the resultant force and moment on the edge are equal to zero. The bending moments are opposed by bulk moments of the plate represented as the plate flexural rigidity D. Since this approximation accurately predicts plate bending behavior away from the boundary areas,[24] the deflections are measured at the plate center $(r=0)$.

The total plate deflection w_m has two terms: one term due to an initial deflection w_δ, and an additional term Δw due

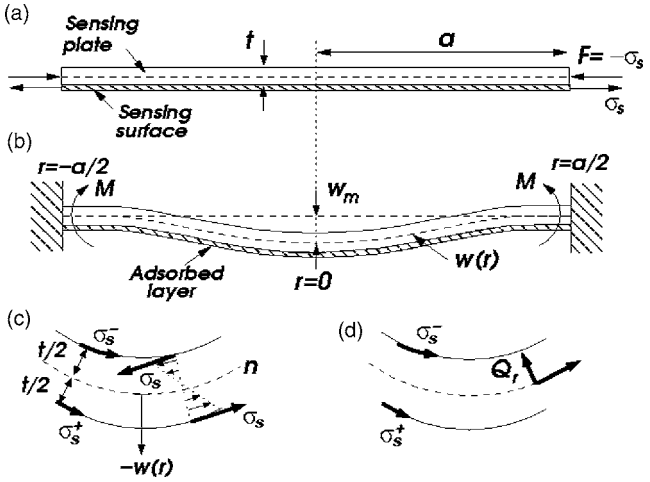

FIG. 1. (a) Dimensions and forces, (b) plate bending due to σ_s (compressive in this case), (c) σ_s generates a bending couple M, and (d) shear force Q_r generated by large displacements.

[a]Electronic mail: e.t.carlen@ewi.utwente.nl

 © 2006 American Institute of Physics
Downloaded 27 Oct 2006 to 130.89.29.56. Redistribution subject to AIP license or copyright, see http://apl.aip.org/apl/copyright.jsp

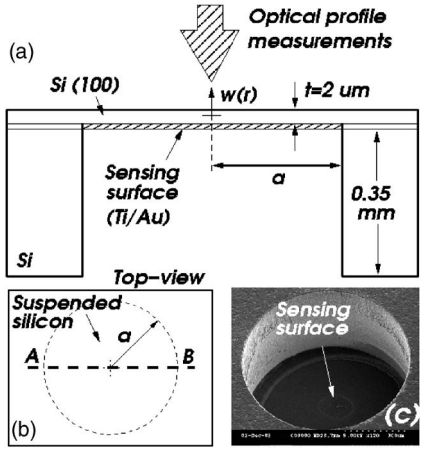

FIG. 2. (a) Device cross section used for optical interferometry measurements, (b) plate deflection profiles from line *A*-*B*, and (c) scanning electron microscopy of exposed sensing surface before Ti/Au sputtering.

to the radial surface force induced by the adsorption on the sensing surface. In practice, suspended silicon plates are rarely perfectly flat for a variety of reasons including imperfections of the silicon layer, a thin stressed film or adsorbed species on the plate surface, or deflections due to gravity. All suspended plates fabricated to date have initial plate bending due primarily to the residual stress in the nucleation layer.[25] Since w_δ is much larger than Δw ($w_\delta \sim 10\times\Delta w$), then w_δ must be considered when calculating the change in differential surface stress $\Delta\sigma_s$. For a circular plate with clamped edges, the initial deflection is $w_i(r)=w_\delta(1-r^2/a^2)^2$,[26] where a is the plate radius and w_δ is the maximum initial deflection (at $r=0$). The total deflection due to the combined effects of initial bending and a compressive surface stress is $w(r)=[32w_\delta/(\beta a)^2][(J_0(\beta r)-J_0(\beta a))/(\beta a)J_1(\beta a)-(1/2)(1-r^2/a^2)]$,[27] where J_0 and J_1 are Bessel functions of the first kind, $\beta^2=\sigma_s/D$, $D=E(1-\nu^2)^{-1}t^3/12$, E the elasticity modulus, and ν the Poisson ratio. The change in differential surface stress is then $\Delta\sigma_s \approx (80/11)\gamma(1+(w_\delta(w_\delta+4\Delta w))^{1/2}w_\delta^{-1})$,[28] where $w_\delta<0$, $\gamma=D/a^2$, and $\Delta\sigma_s=(\sigma_s)_{t=t_f}-(\sigma_s)_{t=0}$ assuming $(\sigma_s^-)_{t=t_f}\approx(\sigma_s^-)_{t=0}$. For applications such as label-free biosensing, the precise calculation of the binding induced surface stress change may not be necessary; however, choosing a receptor layer with the appropriate functional group that generates a large change in surface stress upon binding is essential to maximize the signal-to-noise ratio.

Microfabricated suspended silicon plates are used to demonstrate the bending behavior induced by the vapor phase chemisorption of the alkanethiol monolayers, shown in Fig. 2(a). Structures were fabricated using a conventional surface micromachining process,[29] requiring two contact lithography steps. First, the device layer of the silicon-on-insulator substrate is defined and reactive-ion etched defining the sensing plate. The back of the substrate is patterned with holes aligned to the sensing plate, and the silicon substrate removed using a reactive-ion etch step. The plate radius is reduced due to an 87° sidewall slope following the substrate etch step. The remaining oxide layer is removed in a 3:1 $HF:H_2O$ solution.

Self-assembling alkanethiol monolayers on Au(111) nucleation layers are used for plate bending characterization. Alkanethiols are highly ordered and stable molecular monolayers that organize on gold surfaces.[30–32] The high affinity of thiols for gold surfaces provides an attractive medium to generate well-defined organic surfaces with a wide range of chemical functionalities displayed at the sensing interface. The bottom side of the silicon plates is sputtered coated with a 30 nm Au nucleation layer (with 8 nm Ti adhesion layer), and x-ray diffraction data[33] are shown in Fig. 3(a). Immediately following gold deposition, the initial deflections of the suspended silicon plates are measured, across line *A*-*B* from Fig. 2(b), before exposure to alkanethiol vapor. Figure 3(b) shows an example of the preexposure plate deflection with average center deflection $\langle w_\delta\rangle=-361$ nm from a total of 31 preexposure measurements recorded in 10 s intervals; each measurement is a five-scan average. Surface images mea-

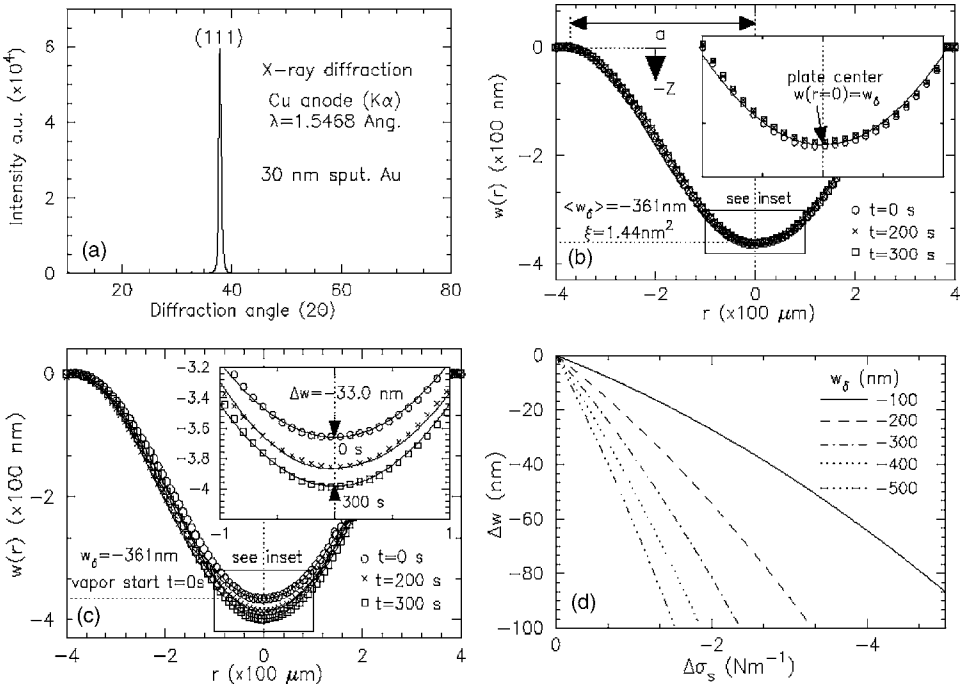

FIG. 3. (a) X-ray diffraction scan 30 nm sputtered Au layer (with 8 nm Ti layer), (b) measured plate bending at $t=0$, 200, and 300 s (10 s intervals) prior to vapor exposure, (c) bending during 1-dodecanethiol vapor exposure: $(\Delta\sigma_s)_{200\ s}=0.45$ N m^{-1} and $(\Delta\sigma_s)_{300\ s}=0.72$ N m^{-1}, and (d) calculated Δw as a function of $\Delta\sigma_s$ and w_δ. $T\approx 25$ °C and $RH\approx 50\%$. All calculations use $a=380$ μm, $t=2$ μm, $E=150$ GPa, and $\nu=0.2$.

Downloaded 27 Oct 2006 to 130.89.29.56. Redistribution subject to AIP license or copyright, see http://apl.aip.org/apl/copyright.jsp

sured with a phase scanning interferometric optical profilometer ($\lambda=631$ nm; 20× objective; Wyko, model: RST Plus). The plate surfaces are then exposed to vapor phase (as received) 1-dodecanethiol [$CH_3-(CH_2)_{11}-SH$, ⩾98% Aldrich No. 471364] from a large reservoir of liquid solution ≈400 μl, for 300 s. Figure 3(c) shows the plate deflection change at three different measurement times $t=0$, 200, and 300 s, each recorded in 10 s and a five-scan average. The increased deflection in the $-Z$ direction indicates a compressive differential surface stress. The saturated center deflection is $\Delta w=-33$ nm, consistent with measurements on different structures. The calculated saturated surface stress of the chemisorbed 1-dodecanethiol monolayer is $\Delta\sigma_s=-0.72\pm0.02$ N m^{-1}, larger than -0.2 N m^{-1} reported by Berger *et al.*,[10] but close to -0.52 ± 0.01 N m^{-1} reported by Godin *et al.*[12] The compressive surface stress change indicates that the Au(111) surface free energy has been reduced through the chemisorption of the methyl-terminated alkanethiol. Figure 3(d) shows the variation of the surface stress induced plate deflection with different initial plate deflections, demonstrating the dependence of Δw on different values of w_δ.

The microfabricated surface stress plate sensors presented here are advantageous compared to cantilever beam structures in two important ways. (a) Plate structures are more rigid than beams with effective spring constants in the range of 50–100 N m^{-1} and therefore can be easily functionalized and probed using commercially available printing techniques. (b) The detection surface is physically isolated from the sensing surface and therefore can be easily adapted to other readout techniques in liquid solutions, such as a differential capacitance synchronous demodulation technique with reported displacement measurement resolution ≈210 fm (1 Hz bandwidth).[34] Although the ratio of deflection to surface stress ($\eta=\Delta w/\Delta\sigma_s$) for cantilever beams is typically larger than the plate structures by a factor of ≈10–100×,[35] the electronic displacement detection resolution exceeds that of reported optical detection techniques[36,37] by ≈10–100×,[38] suggesting that the plate structures with electronic readout are as sensitive as the cantilever beam-optical readout systems.

The authors thank The Charles Stark Draper Laboratory for research funding, and Connie Cardoso, Mert Prince, and Manuela Healey for fabrication assistance.

[1]H. Ibach, Surf. Sci. Rep. **29**, 193 (1997).
[2]D. Sander, Curr. Opin. Solid State Mater. Sci. **7**, 51 (2003).
[3]J. Cahn and R. Hanneman, Surf. Sci. **1**, 387 (1964).
[4]L. Jaeckel, G. Láng, and K. Heusler, Electrochim. Acta **39**, 1031 (1994).
[5]R. W. Hoffman, in *Physics of Thin Films*, edited by G. Hass and R. E. Thun (Academic, New York, 1966), Vol. 3, pp. 211.
[6]A. Moulin, S. O'Shea, R. Badley, P. Doyle, and M. Welland, Langmuir **15**, 8776 (1999).
[7]G. Wu, R. Dat, K. Hansen, T. Thundat, R. Cote, and A. Majumdar, Nat. Biotechnol. **19**, 856 (2001).
[8]J. Pei, F. Tian, and T. Thundat, Anal. Chem. **76**, 292 (2004).
[9]H.-J. Butt, J. Colloid Interface Sci. **180**, 251 (1996).
[10]R. Berger, E. Delamarche, H. Lang, C. Gerber, J. Gimzewski, E. Meyer, and H.-J. Güntherodt, Science **276**, 2021 (1997).
[11]R. Raiteri, H.-J. Butt, and M. Grattarola, Scanning Microsc. **12**, 243 (1998).
[12]M. Godin, P. Williams, V. Tabard-Cossa, O. Laroche, L. Beaulieu, R. Lennox, and P. Grütter, Langmuir **20**, 7090 (2004).
[13]K. Marx, Biomacromolecules **4**, 1099 (2003).
[14]T. Thundat, E. Wachter, S. Sharp, and R. Warmack, Appl. Phys. Lett. **66**, 1695 (1995).
[15]B. Ilic, D. Czaplewski, H. Craighead, P. Neuzil, C. Campagnolo, and C. Batt, Appl. Phys. Lett. **77**, 450 (2000).
[16]J. Tamayo, A. Humphris, A. Malloy, and M. Miles, Ultramicroscopy **86**, 167 (2001).
[17]T. Burg and S. Manalis, Appl. Phys. Lett. **83**, 2698 (2003).
[18]R. Shuttleworth, Proc. Phys. Soc., London, Sect. A **63**, 444 (1950).
[19]P. Couchman, W. Jesser, and D. Kuhlmann-Wilsdorf, Surf. Sci. **33**, 429 (1972).
[20]S. Timoshenko, *Theory of Plates and Shells* (McGraw-Hill, New York, 1959), p. 333.
[21]For all devices tested, (a) nominal plate thickness $t=2$ μm, (b) $t=d/400$, and (c) $w_m\leqslant t/5$. Szilard (Ref. 23) recommends $t/10\leqslant w_m\leqslant t/5$.
[22]Defined as tension for $\sigma_s>0$ and compression for $\sigma_s<0$.
[23]R. Szilard, *Theory and Analysis of Plates: Classical and Numerical Methods* (Prentice-Hall, Englewood Cliffs, NJ, 1974), p. 28.
[24]S. P. Timoshenko and J. N. Goodier, *Theory of Elasticity*, 3rd ed. (McGraw-Hill, New York, 1970), 39.
[25]Average residual stress of Ti/Au (8 nm/30 nm) layers measured (FLX-2320-S, Toho Technology Corp.) in separate experiments on 100 mm diameter silicon wafers (average of five measurements) with average compressive stress of -181 MN m^{-2}.
[26]R. Szilard, *Theory and Analysis of Plates: Classical and Numerical Methods* (Prentice-Hall, Englewood Cliffs, NJ, 1974), p. 97.
[27]A solution of $(d^3w/dr^3)+(1/r)(d^2w/dr^2)-((\sigma_s/D)+(1/r^2))(dw/dr)-p_0r/2D=0$ with boundary conditions $w=dw/dr=0$ at $r=\pm a/2$. The variable p_0 represents a uniform lateral pressure (Ref. 26) and is calculated by assuming that the initial bending is identical to the bending due to p_0. The center deflection due to p_0, $w_i(0)=p_0a^4/64D$, (Ref. 26), is equated to the initial bending $w_i(0)$ resulting in $w_\delta=p_0a^4/64D$ and $p_0=64Dw_\delta/a^4$. The term $p_0r/2D$ is then replaced with $32w_\delta r/a^4$.
[28]Deflection $\Delta w=w(0)-w_i(0)\approx w_\delta(5/72\gamma^{-1}\Delta\sigma_s+11/2304\gamma^{-2}\Delta\sigma_s^2)$, where $w(0)$ replaced with first three terms of series expansion. The quadratic equation is solved for $\Delta\sigma_s$.
[29]W. Sawyer, M. Prince, and G. Brown, J. Micromech. Microeng. **15**, 1588 (2005).
[30]R. Nuzzo and D. Allara, J. Am. Chem. Soc. **105**, 4481 (1983).
[31]R. Nuzzo, B. Zegarski, and L. Dubois, J. Am. Chem. Soc. **109**, 733 (1987).
[32]C. Bains, E. Troughton, Y.-T. Tao, J. Evall, G. Whitesides, and R. Nuzzo, J. Am. Chem. Soc. **111**, 321 (1989).
[33]Peak occurs at $2\theta=37.94°$ corresponding to the (111) direction for Au.
[34]J. Doscher, Analog Dialogue **33**, 27 (1999).
[35]Comparison between cantilever beam dimensions from Refs. 6–10 and plate dimensions presented here.
[36]D. Rugar, H. Mamin, and P. Guethner, Appl. Phys. Lett. **55**, 2588 (1989).
[37]G. Yaralioglu, A. Atalar, S. Manalis, and C. Quate, J. Appl. Phys. **83**, 7405 (1998).
[38]A displacement resolution of 0.001 nm reported (Ref. 36) using optical interferometry; however, a value of 0.01 nm is common (Ref. 37).

Downloaded 27 Oct 2006 to 130.89.29.56. Redistribution subject to AIP license or copyright, see http://apl.aip.org/apl/copyright.jsp